Appl. Math. J. Chinese Univ.
2014, 29(4): 379-390

Discussion on relationship between minimal energy and curve shapes

LI Xue-mei[1] ZHANG Yong-xia[1] MA Long[1] ZHOU Yuan-feng[1]
ZHANG Cai-ming[1,2]

Abstract. Energy minimization has been widely used for constructing curve and surface in the fields such as computer-aided geometric design, computer graphics. However, our testing examples show that energy minimization does not optimize the shape of the curve sometimes. This paper studies the relationship between minimizing strain energy and curve shapes, the study is carried out by constructing a cubic Hermite curve with satisfactory shape. The cubic Hermite curve interpolates the positions and tangent vectors of two given endpoints. Computer simulation technique has become one of the methods of scientific discovery, the study process is carried out by numerical computation and computer simulation technique. Our result shows that: (1) cubic Hermite curves cannot be constructed by solely minimizing the strain energy; (2) by adoption of a local minimum value of the strain energy, the shapes of cubic Hermite curves could be determined for about 60 percent of all cases, some of which have unsatisfactory shapes, however. Based on strain energy model and analysis, a new model is presented for constructing cubic Hermite curves with satisfactory shapes, which is a modification of strain energy model. The new model uses an explicit formula to compute the magnitudes of the two tangent vectors, and has the properties: (1) it is easy to compute; (2) it makes the cubic Hermite curves have satisfactory shapes while holding the good property of minimizing strain energy for some cases in curve construction. The comparison of the new model with the minimum strain energy model is included.

§1 Introduction

Constructing curves and surfaces with satisfactory shapes is of fundamental importance in computer-aided geometric design, computer graphics and so on[8,10]. A satisfactory curve should satisfy many nice properties, for example, the monotonicity of curvature, symmetry, no undulation (limited number of extremal values of curvature, for cubic Hermite curves, only one extremal value of curvature at most), and the shape suggested by the data points. Energy minimization has been widely used for constructing such curves and surfaces. Some examples are

Received: 2013-10-15.
MR Subject Classification: 37M05, 74G65, 65D17.
Keywords: computer simulation, cubic Hermite curve, minimum strain energy, curve shape.
Digital Object Identifier(DOI): 10.1007/s11766-014-3230-2.
Supported by the National Natural Science Foundation of China (61173174, 61103150, 61373078), the NSFC Joint Fund with Guangdong under Key Project (U1201258), and the National Research Foundation for the Doctoral Program of Higher Education of China (20110131130004).

as follows. In physics-based deformation, physical simulation is used to get realistic shapes and motions, the final surface is produced by the equilibrium state of the dynamic model[2,12]. In constrained deformation, the shape of a surface is faired by minimizing a global energy[3,14,17]. In the construction of minimal-energy spline segments and curves with angle constraints, the existence of solutions has been proved, the Lagrange multiplier rules has been justified, and some nice properties have been obtained[5]. The use of energy integral in optimizing the 'fairness' of PH curve and geometric Hermite interpolants was discussed[6,9], and compelling empirical evidence indicates that, for 'reasonable' derivative data, first-order PH quintic Hermite interpolants are systematically of lower energy than their ordinary cubic counterparts. Constrained shape scaling of a surface is like the manipulation of a thin plate. When external forces such as moment, edge force and gravity either do not exist, the potential energy of the free plate[11] includes bending strain energy, stretching strain energy[7,13] and spring potential energy. Hence, the constrained shape scaling of a surface could be simplified to the *stretching* problem, the resulting surface is obtained by minimizing the weighted combination of three energies, that is, bending strain energy, the stretching strain energy and the spring potential energy[16].

The polynomial interpolation process is commonly used in curve construction, and generally the resulting polynomial curve is either a cubic Hermite curve or a cubic Bézier curve. The constructed curve is required to have nice properties or desirable shapes suggested by the interpolation conditions. The standard cubic polynomial technique has been addressed in paper[1], where so called geometric cubic Hermite(GCH) curves are constructed, which interpolates the given positions and tangent vectors at the two end-points. The curves of this type allow flexibility on the magnitudes of the two tangent vectors. Yong and Cheng[15] propose a solution to the construction of G^1 GCH curves. The curve is built by optimizing the magnitudes of tangent vectors at endpoints; the strain energy of the curve is thus minimized. An explicit formula for obtaining such a curve is also presented in that paper. A method[4] is proposed to construct shape pleasing GCH curves, where curvature variation is used as an objective function. An explicit formula for obtaining such a curve is given. However, GCH curves by the methods[4,15] are composed of two or three parts for some input; and their shapes are not always good.

It is generally accepted that a curve would have a desirable shape if it has the minimum internal strain energy. This paper tests the shape of a curve with minimum strain energy, and GCH curve is used in the test process. The shape of the GCH curve is determined by minimizing the strain energy. As the curve of this type interpolates the given positions and tangent vectors at two endpoints, minimizing the strain energy is a task of determining the magnitudes of the two tangent vectors. The numerical computation and computer simulation techniques are used to compute the minimum strain energy and visualize the magnitudes of the two tangent vectors. Our results show that minimizing the strain energy cannot guarantee the cubic curve with a satisfactory shape, using the local minimum strain energy to construct GCH curves, the shapes of constructed curves are satisfactory for most cases. Based on the strain energy model and computing results, a new explicit model is presented for constructing GCH curve with satisfactory shape. The new model has the property that it is very simple and suitable for constructing cubic polynomial curve with satisfactory shape.

The remaining part of the paper is arranged as follows. Section 2 is the discussion on curve shapes and the minimum strain energy. Section 3 presents the construction of the new model. Section 4 shows the comparison of the new method with minimizing strain energy model. Finally section 5 concludes the paper.

§2 Curve shape and minimum strain energy

In this section, the cubic Hermite curve is used to test the relationship between minimum strain energy and the shape of a curve.

2.1 Construction of cubic Hermite curve

Given four interpolation conditions which are two points $P_0 = (0, 0)$ and $P_1 = (1, 0)$, and two tangent vectors $V_0 = (\cos\theta, \sin\theta)$ and $V_1 = (\cos\varphi, \sin\varphi)$ at P_0 and P_1, respectively, where θ denotes the angle from vector P_0P_1 to V_0, φ the one from vector P_0P_1 to V_1, as shown in Fig. 1. The cubic Hermite curve $P(t)$ that matches the four interpolation conditions can be defined by

$$P(t) = P_0F_0(t) + \alpha V_0G_0(t) + \beta V_1G_1(t) + P_1F_1(t) \tag{1}$$

where

$$F_0(t) = 2t^3 - 3t^2 + 1, \quad F_1(t) = -2t^3 + 3t^2$$
$$G_0(t) = t^3 - 2t^2 + t, \quad G_1(t) = t^3 - t^2$$

are cubic Hermite basis functions on [0,1], α and β are magnitudes of V_0 and V_1, and will be determined.

Figure 1: Four interpolation conditions

As α and β are variable, $P(t)$ has different shapes with different (α, β). For example, in $P(t)$ (1), let $V_0 = (\sqrt{2}/2, \sqrt{2}/2)$ and $V_1 = (\sqrt{2}/2, -\sqrt{2}/2)$, then, its plots for $(\alpha, \beta) = \{(2, 2), (1, 4), (3.2, 8.5), (6, 7)\}$ are shown in Fig. 2.

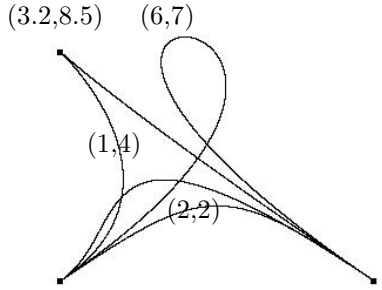

Figure 2: plots of $P(t)$ with different (α, β)

The vectors V_0 and V_1 are functions of θ and φ, respectively. The goal is that for a given (θ, φ), a suitable (α, β) is chosen so that $P(t)$ (1) satisfies the given interpolation conditions and has a satisfactory shape. Hence, constructing $P(t)$ (1) becomes the problem of constructing the following function

$$\begin{matrix} \alpha = \alpha(\theta, \varphi) \\ \beta = \beta(\theta, \varphi) \end{matrix} \qquad -\pi \le \theta, \varphi \le \pi. \tag{2}$$

It is generally accepted that $P(t)$ (1) would have a satisfactory shape if it has the minimum strain energy. For a given (θ, φ), let $P'(t, \alpha, \beta)$ and $P''(t, \alpha, \beta)$ denote the first and second derivatives of $P(t)$ (1) with respect to t, the strain energy of $P(t)$ is defined by

$$G(\alpha, \beta) = \int_0^1 \frac{|P'(t, \alpha, \beta) \times P''(t, \alpha, \beta)|^2}{|P'(t, \alpha, \beta)|^5} dt \tag{3}$$

then, for the given (θ, φ), the values of α and β will be determined by minimizing $G(\alpha, \beta)$, i.e., they are determined by

$$\frac{\partial G(\alpha, \beta)}{\partial \alpha} = 0, \qquad \frac{\partial G(\alpha, \beta)}{\partial \beta} = 0 \tag{4}$$

that is, function (2) is defined by (4).

In the following subsection, we will discuss the relationship between the shape of $P(t)$ (1) and (α, β) defined by (4).

2.2 Curve shape and minimum strain energy

Using numerical computing and computer simulation techniques, we can define $P(t)$ (1) by computing the minimum energy value of $P(t)$ to obtain α and β. The process of computing the minimum energy value of $P(t)$ is as follows. The region of (θ, φ), $-\pi \le \theta, \varphi \le \pi$, is subdivided into 100×100 small squares meshes using (θ_i, φ_j) which are defined by

$$\theta_i = \frac{i\pi}{50} - \pi, \qquad \varphi_j = \frac{j\pi}{50} - \pi,$$

for $i, j = 0, 1, 2, \cdots, 100$. For each (θ_i, φ_j), the minimum energy value of $P(t)$ is computed by subdivision method, that is, the region $0 \le \alpha, \beta \le \Delta$ is subdivided into 100×100 small squares using $(\alpha_i, \beta_j) = (\Delta i/100, \Delta j/100)$, $i, j = 0, 1, 2, \cdots, 100$. For $(\alpha_i, \beta_j) = (i, j)$, $i, j = 0, 1, 2, \cdots, 100$, if $P(t)$ has the least energy value at $(\alpha_{i0}, \beta_{j0})$, then sub-square $[\alpha_{i0} - L \le \alpha \le \alpha_{i0} + L] \times [\beta_{j0} - L \le \beta \le \beta_{j0} + L]$ with $L = \Delta/100$ is subdivided into 100×100 small squares, repeating the above process until the side length of the current small square less than a given small value. In our experiment, Δ is taken as 100, we have not found the case that when $\alpha > 100$ or $\beta > 100$, $P(t)$ has the minimum energy value. The computing and simulation results are that minimizing the strain energy does not guarantee $P(t)$ (1) to have satisfactory shape, and for $-\pi \le \theta, \varphi \le \pi$, $G(\alpha, \beta)$ (3) can be classified into the following two cases:

1. when (θ, φ) does not belong to the dotted region in Fig. 3, $G(\alpha, \beta)$ has one local minimum value and one minimum value zero when $\alpha \to \infty$ and $\beta \to \infty$.

2. when (θ, φ) belongs to the dotted region in Fig. 3, $G(\alpha, \beta)$ has no local minimum value, and one minimum value zero when $\alpha \to \infty$ and $\beta \to \infty$.

Figures 4 - 5 are two examples corresponding to the above two cases, for simplicity, we set $\alpha = \beta$. In Fig. 4, $V_0 = (\cos\frac{\pi}{3}, \sin\frac{\pi}{3})$ and $V_1 = (\cos\frac{-\pi}{3}, \sin\frac{-\pi}{3})$, the plot on the top is the curve (with $\alpha = 1.43$) that has local minimum energy $G(1.43, 1.43) = 3.6$, the plot at the bottom is the energy curve of $G(\alpha, \alpha)$ that has the properties that 1) when $\alpha = 6$, $G(\alpha, \alpha) \to \infty$ and $P(t)$ (1) have one cusp; 2) when $\alpha \to \infty$, $G(\alpha, \alpha) \to 0$. In Fig. 5, $V_0 = (\cos\frac{-3\pi}{4}, \sin\frac{-3\pi}{4})$ and $V_1 = (\cos\frac{3\pi}{4}, \sin\frac{3\pi}{4})$, the plot on the top is the curve (with $\alpha = 2$), the plot at the bottom is the energy curve of $G(\alpha, \alpha)$ that has no local minimum, and when $\alpha \to \infty$, $G(\alpha, \alpha) \to 0$.

The case in Figure 5 shows that with constraint (4), $P(t)$ (1) could not be defined for any (θ, φ). The following discussion will show that with (α, β) being defined by the local minimum value of $G(\alpha, \beta)$, $P(t)$ (1) could be defined for many cases, but may not have satisfactory shape in some cases.

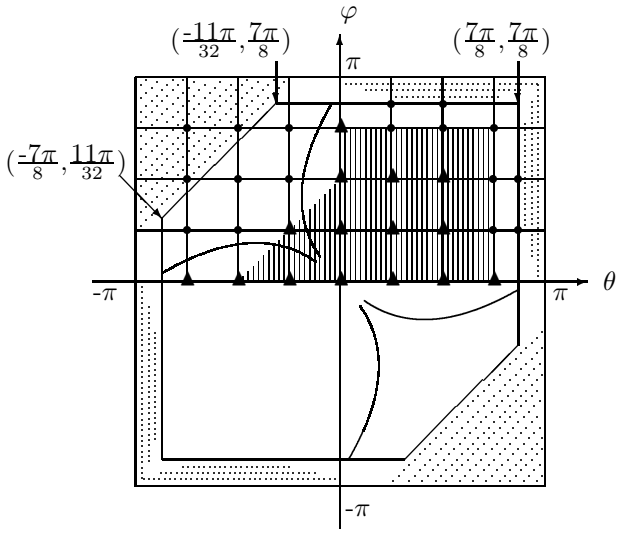

Figure 3: The region for constructing (α, β) in (2)

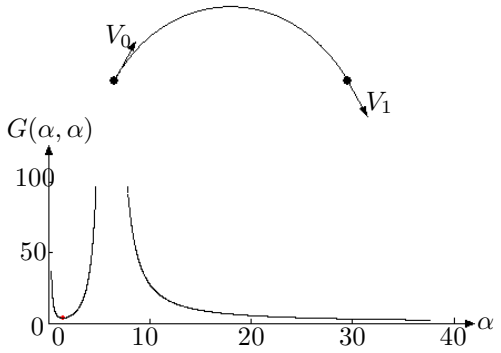

Figure 4: Interpolation curve and energy curve

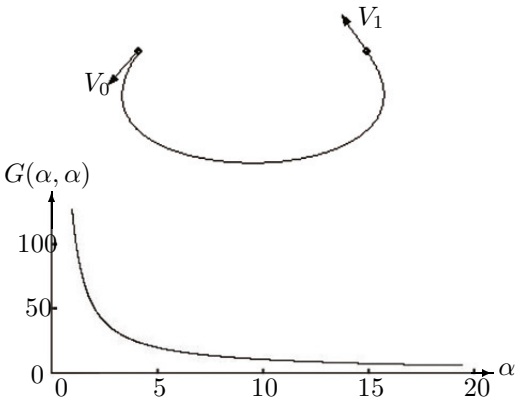

Figure 5: Interpolation curve and energy curve

2.3 Curve shape and local minimum strain energy

When (θ, φ) does not belong to the dotted region in Fig. 3, there is only one (α, β) to make $G(\alpha, \beta)$ reach its local minimum value, the relations of $G(\alpha, \beta)$ and (θ, φ), the surfaces α and β (2) are shown in Figures (6)-(8). It follows from Figures (6)-(8) that

1. $G(\alpha, \beta)$ changes smoothly with the change of (θ, φ);
2. On the region that is not on or close to the four curves in Fig. 3, the values of α and β change smoothly with the smooth change of (θ, φ).
3. On the region that is on or close to the four curves in Fig. 3, the values of α and β do not change smoothly with the smooth change of (θ, φ).

It is clear that for the (θ, φ) which is on or close to the region marked by the four curves in Fig. 3, if the corresponding α and β are defined by the two surfaces in Figures 7 and 8,

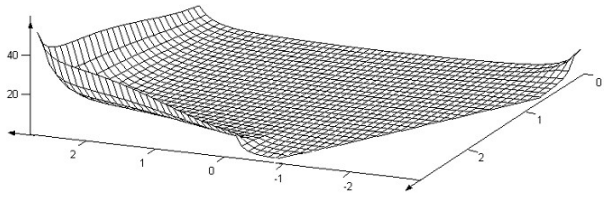

Figure 6: Energy surface

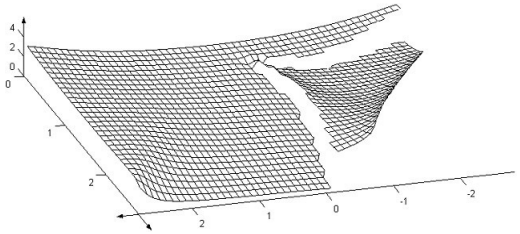

Figure 7: Surface $\alpha = \alpha(\theta, \varphi)$

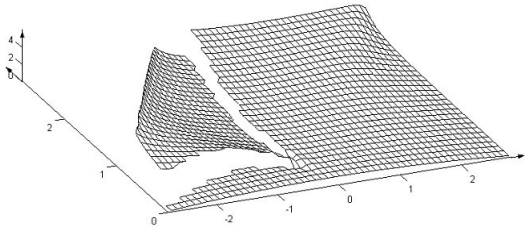

Figure 8: Surface $\beta = \beta(\theta, \varphi)$

respectively, then $P(t)$ (1) could not have satisfactory shape, as close to the region marked by the four curves, (α, β) has a jump change so that the shape of $P(t)$ (1) has a jump change. This means that the shape of $P(t)$ (1) is not satisfactory on the region before jump change or after jump change at least. For example, Figures 9- 11 are the energy curve $G(\alpha, \beta)$, α curve and β curve, for $-6\pi/32 \le \theta \le 1\pi/32$, $\varphi = 23\pi/32$, respectively, which are obtained by constraint (4). The curve $G(\alpha, \beta)$ in Fig. 9 changes smoothly. While in Figures 10-11, the curves $\alpha(\theta, 23\pi/32)$ and $\beta(\theta, 23\pi/32)$ corresponding to $G(\alpha, \beta)$ in Fig. 9 do not change smoothly, each of which has jump change. Fig. 12 is the plots of the eight cubic Hermite curves, the values of α and β of the eight curves are taken from the two curves (in Figures 10-11) at the positions marked by the red symbol $\bullet$, and the green symbol $\bullet$ denotes the jump point. It's clear that with the uniform change of θ, the shapes of the curves don't change smoothly, the shapes of curves (d) and (e) are obviously different. For more precise, Fig. 13 has two plots of the curves C_l with $\theta_l = -0.2774439$(left curve) and C_r with $\theta_r = -0.2774438$(right curve), the difference between θ_l and θ_r is 0.0000001, but the shapes of C_l and C_r are obviously different, so there is at least one of the two curves to be of unsatisfactory shape, or both are of unsatisfactory shape.

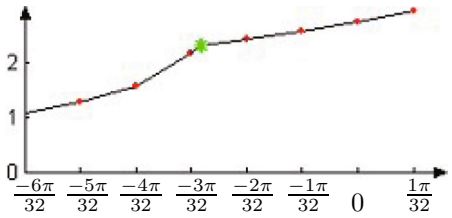

Figure 9: Plot of $G(\alpha, \beta)$ for $\frac{-6\pi}{32} \le \theta \le \frac{1\pi}{32}$, $\varphi = \frac{23\pi}{32}$

The above discussion shows that minimizing the strain energy (3) could not make $P(t)$ (1) have a satisfactory shape. So in the following section, we will discuss the construction of a new model to compute α and β so that $P(t)$ (1) has a satisfactory shape.

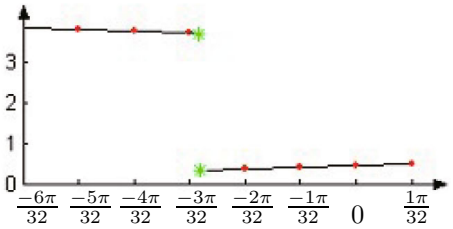

Figure 10: Plot of $\alpha(\theta, \frac{23\pi}{32})$ for $\frac{-6\pi}{32} \le \theta \le \frac{1\pi}{32}$

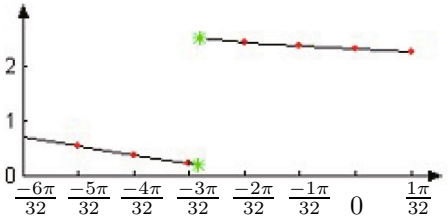

Figure 11: Curve $\beta(\theta, \frac{23\pi}{32})$ for $\frac{-6\pi}{32} \le \theta \le \frac{1\pi}{32}$

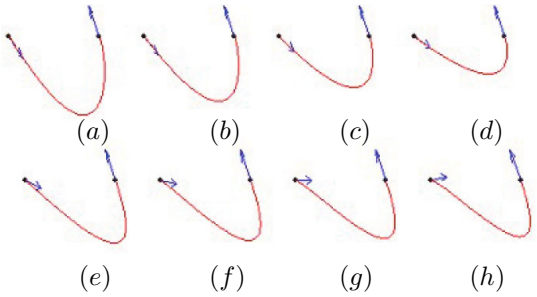

Figure 12: Cubic Hermite curves

Figure 13: Two curves with $\theta_l = -0.2774439$ and $\theta_r = -0.2774438$

§3 Construction of new model

The new model which will be constructed is defined as

$$\begin{matrix} \bar{\alpha} = \bar{\alpha}(\theta, \varphi) \\ \bar{\beta} = \bar{\beta}(\theta, \varphi) \end{matrix} \qquad -\pi \le \theta, \varphi \le \pi \tag{5}$$

On the first, second, third and fourth quadrant, $\bar{\alpha}(\theta, \varphi)$ and $\bar{\beta}(\theta, \varphi)$ are denoted by $\bar{\alpha}_i(\theta, \varphi)$ and $\bar{\beta}_i(\theta, \varphi)$, $i = 1, 2, 3, 4$, respectively. Based on Fig. 1−3, as symmetry, $\bar{\alpha}(\theta, \varphi)$ and $\bar{\beta}(\theta, \varphi)$ in (5) satisfy the following relation

- On the first quadrant, $\bar{\alpha}_1(\theta, \varphi) = \bar{\beta}_1(\varphi, \theta)$;
- On the second quadrant, $\bar{\alpha}_2(\theta, \varphi) = \bar{\beta}_2(-\varphi, -\theta)$;
- On the third quadrant, $\bar{\alpha}_3(\theta, \varphi) = \bar{\alpha}_1(-\theta, -\varphi)$ and $\bar{\beta}_3(\theta, \varphi) = \bar{\beta}_1(-\theta, -\varphi)$;
- On the fourth quadrant, $\bar{\alpha}_4(\theta, \varphi) = \bar{\alpha}_2(-\theta, -\varphi)$ and $\bar{\beta}_4(\theta, \varphi) = \bar{\beta}_2(-\theta, -\varphi)$.

Hence, we only need to discuss the construction of $\bar{\alpha} = \bar{\alpha}(\theta, \varphi)$ on the first and the second quadrants.

The computing and simulation results showed that a) when (θ, φ) belongs to the vertical line region in Fig. 3, the shapes of $P(t)$'s (1) which are defined by (4) are fine. Note that although $\alpha = \alpha(\theta, \varphi)$ has jump on the vertical line region in the second quadrant, the jump is small; b) in the second quadrant, with the (θ, φ) being farther and farther away from the vertical line region in Fig. 3, the shapes of $P(t)$'s (1) which are defined by (4) are getting worse. For example(as symmetry, the curves for $(\theta, \varphi) = (\pi/N, -\pi/N)$ and $(-\pi/N, \pi/N)$ have the same shape), the curve for $(\theta, \varphi) = (\pi/4, -\pi/4)$ which is given in Fig. 38) of Appendix has satisfactory shape, while the one for $(\theta, \varphi) = (\pi/2, -\pi/2)$ in Fig. 45) of Appendix (red curve)

does not have satisfactory shape. To make the cubic Hermite curves have satisfactory shapes while holding the good property of minimizing strain energy, $\bar{\alpha_1} = \bar{\alpha}_1(\theta, \varphi)$ and $\bar{\alpha_2} = \bar{\alpha}_2(\theta, \varphi)$ are constructed by the way that, on the vertical line region in Fig. 3, $\bar{\alpha}_1$ and $\bar{\alpha}_2$ approximate α in (2), on the other region, $\bar{\alpha}_1$ and $\bar{\alpha}_2$ are defined by making $P(t)$ (1) have satisfactory shape.

For constructing $\bar{\alpha_1} = \bar{\alpha}_1(\theta, \varphi)$ and $\bar{\alpha_2} = \bar{\alpha}_2(\theta, \varphi)$, the two special cases are considered firstly.

1. When $\theta = \varphi = 0$, the solution of α and β is not unique, any $\alpha > 0$ and $\beta > 0$ satisfy equation (4). In this case, the best choice is to set $\alpha = \beta = 1$, this choice makes $P(t)$ (1) be a straight line with the magnitude of the first derivative being one constant. Such a straight line is the most naturally defined curve one can get in this case.

2. For $\theta = \pi/2$ and $\varphi = -\pi/2$, the best choice is to set $\alpha = \beta = 2$, this choice makes $P(t)$ (1) have the satisfactory shape. For example, in Fig. 45) in Appendix, the red curve $P(t)$ (1) and its curvature are produced by minimizing the strain energy, the blue curve $P(t)$ (1) and its curvature are produced by setting $\alpha = \beta = 2$. For the blue curve, $P(1/2) = (1/2, 1/2)$ and the middle point of the curve is coincide with the corresponding middle point of the half circle. In this case, $P(t)$ (1) can be regarded as an approximation of half circle.

Now, based on the above discussion, the process of constructing $\bar{\alpha_1} = \bar{\alpha}_1(\theta, \varphi)$ and $\bar{\alpha_2} = \bar{\alpha}_2(\theta, \varphi)$ is described in detail as follows. First, the values of α at the positions marked by the symbol ▲ are produced by (4), the ones of α at the positions marked by the symbol • are produced by Human-Computer Interaction to make the shapes of the curves fine, then, $\bar{\alpha_1} = \bar{\alpha}_1(\theta, \varphi)$ and $\bar{\alpha_2} = \bar{\alpha}_2(\theta, \varphi)$ are constructed by interpolating the values at positions marked by symbols ▲ and •. Now $\bar{\alpha}_1(\theta, \varphi)$ and $\bar{\alpha}_2(\theta, \varphi)$ are defined by

$$\bar{\alpha}_1(\theta, \varphi) = [f_0(\theta)\ f_1(\theta)\ f_2(\theta)\ f_3(\theta)]\, E_1 \left[\ f_0(\varphi)\ f_1(\varphi)\ f_2(\varphi)\ f_3(\varphi)\ \right]^T \tag{6}$$

$$\bar{\alpha}_2(\theta, \varphi) = [f_0(\theta)\ f_1(\theta)\ f_2(\theta)\ f_3(\theta)]\, E_2 \left[\ f_0(\varphi)\ f_1(\varphi)\ f_2(\varphi)\ f_3(\varphi)\ \right]^T \tag{7}$$

where

$$E_1 = \begin{bmatrix} 1 & 0.93 & 0.737 & 0.403 \\ 1.13 & 1.16 & 0.992 & 0.579 \\ 1.578 & 1.628 & 1.645 & 0.971 \\ 2.453 & 2.314 & 2.445 & 1.867 \end{bmatrix} \quad \text{and} \quad E_2 = \begin{bmatrix} 1 & 0.93 & 0.737 & 0.403 \\ 1.13 & 1.209 & 2.67 & 3.825 \\ 1.578 & 0.968 & 2 & 2.120 \\ 2.453 & 0.88 & 3.001 & 3.562 \end{bmatrix}$$

with $f_i(t)$, $(i = 0, 1, 2, 3)$ are basis functions of cubic Lagrange interpolation, where in (6), $f_i(\varphi)$, $i = 0, 1, 2, 3$, are defined on $\varphi_0 = 0$, $\varphi_1 = \pi/4$, $\varphi_2 = \pi/2$ and $\varphi_3 = 3\pi/4$; $f_i(\theta)$, $i = 0, 1, 2, 3$, are defined on $\theta_0 = 0$, $\theta_1 = \pi/4$, $\theta_2 = \pi/2$ and $\theta_3 = 3\pi/4$; while in (7), $f_i(\theta)$, $i = 0, 1, 2, 3$, are defined on $\theta_0 = 0$, $\theta_1 = -\pi/4$, $\theta_2 = -\pi/2$ and $\theta_3 = -3\pi/4$;

§4 Experiment

In this section, the new method (New-M) is compared with the minimizing strain energy model(SE-M)(3) using 63 pairs of (θ, φ) values, which are defined by (θ_i, φ_j), where

$$\begin{array}{l} \theta_i = \frac{i\pi}{8}, \\ \varphi_j = \pm\frac{j\pi}{8} \end{array} \quad i, j = 0, 1, 2, \cdots, 6, 7.$$

In order to avoid repetition, we only draw the curves at points (θ_i, φ_j)s which satisfy

$$\begin{array}{l} \theta_i \geq 0 \ \text{ and } \ \varphi_j \leq \theta_i \quad \text{or} \\ \theta_i \geq 0 \ \text{ and } \ \varphi_j \leq -\theta_i. \end{array}$$

The figures corresponding to (θ_i, φ_j), $i, j = 0, 1, \cdots, 7$ are given in Appendix. The curve for $\theta_0 = \varphi_0 = 0$ does not given as it is a straight line. In each figure of Appendix, the two red curves are produced by SE-M, which are the curve and the curvature of $P(t)$ (1), respectively, while the corresponding two blue curves of $P(t)$ (1) are produced by New-M; The figures in Appendix are divided into three cases:

1. In each of figures $\{1), 2), 4), 6)-9), 11), 13), 15)-20), 22)-27), 29)-37), 39)-48), 51), 52), 57)\}$, the red curve and red curvature are different from the blue ones, where for figures $\{1), 2), 4), 6)-9), 11), 13), 15)-20), 29)-32), 36)\}$, the difference of the blue and red curves are very little and they have visually the same satisfactory shapes; for figures $\{22)-27), 33)-35), 37), 39)-43), 46), 47), 51), 57)\}$, the shapes of blue and red curves are obviously different, but all acceptable; while for figures $\{44), 45), 48), 52)\}$, the blue curves have better shapes than the red ones have.

2. In each of figures $\{3), 5), 10), 12), 14), 21), 38)\}$, the red curves and blue curves coincide, where the blue curves have been covered by the red curves;

3. In each of figures $\{28), 49), 50), 53)-56), 58)-63)\}$, $P(t)$ (1) cannot be produced by SE-M, hence, only the blue curve and curvature are given, the shapes of blue curves are acceptable.

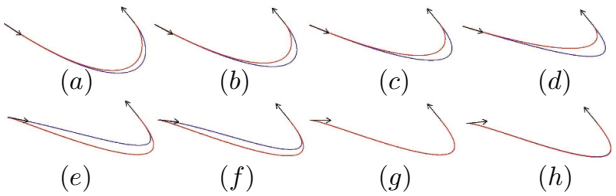

Figure 14: Cubic Hermite curves

Furthermore, for the cases $\theta = \frac{(-6+i)\pi}{32}$, $i = 0, 1, 2, 3, 4, 5, 6, 7$, $\varphi = \frac{23\pi}{32}$ (as shown in Figs. 9-13), the corresponding curves are given in Fig. 14, where the red and blue curves are produced by SE-M and New-M, respectively. The Fig. 14 shows that the blue curves have satisfactory shape and their shapes change smoothly.

The above discussion showed that for some (θ_i, φ_j)s, $P(t)$ (1) cannot be produced by SE-M while for any (θ, φ) satisfying $-\pi \leq \theta, \varphi \leq \pi$, New-M can produce $P(t)$ (1) with satisfactory shape.

§5 Conclusion

Constructing curve and surface by minimizing strain energy is a widely accepted and used approach in CAGD, CG. Our study results show that minimizing strain energy cannot guarantee the cubic Hermite curve to have satisfactory shape. For many cases, minimizing local strain energy can generate cubic Hermite curves with satisfactory shapes. In Fig. 3, however, when (θ, φ) is on or close to the four curves, minimizing local strain energy does not generate cubic Hermite curves with satisfactory shapes. This inspires us to study further how to define the energy to construct curves. We present a new model for constructing satisfactory cubic Hermite curves. The new model is a modification of strain energy model. The experimental results show that the model constructs cubic Hermite curves with satisfactory shapes, when (θ, φ) belongs to

the vertical line region in Fig. 3, the shape of the curve produced by the new model is visually as the same as the one produced by minimizing the exact strain energy.

Our next work is to study the relationship between the shape of a curve(or surface) and other energies such as the stretching strain energy, spring potential energy, the integral of the squared magnitude of the derivative of curvature, the integral of the squared magnitude of the derivative of normal curvature and so on, to get a new effective model for constructing curves with satisfactory shapes.

Appendix

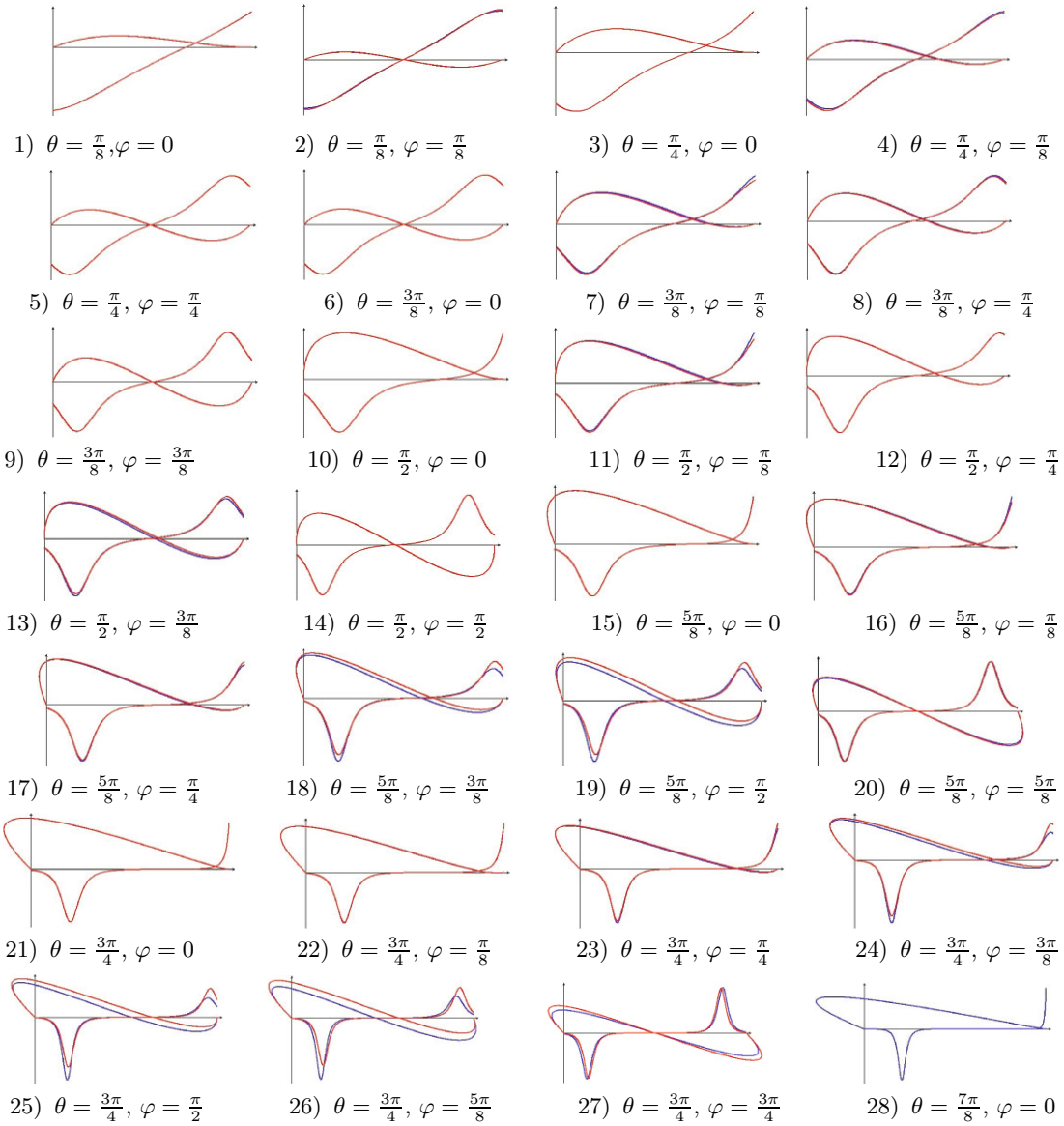

1) $\theta = \frac{\pi}{8}$,$\varphi = 0$ 2) $\theta = \frac{\pi}{8}$, $\varphi = \frac{\pi}{8}$ 3) $\theta = \frac{\pi}{4}$, $\varphi = 0$ 4) $\theta = \frac{\pi}{4}$, $\varphi = \frac{\pi}{8}$

5) $\theta = \frac{\pi}{4}$, $\varphi = \frac{\pi}{4}$ 6) $\theta = \frac{3\pi}{8}$, $\varphi = 0$ 7) $\theta = \frac{3\pi}{8}$, $\varphi = \frac{\pi}{8}$ 8) $\theta = \frac{3\pi}{8}$, $\varphi = \frac{\pi}{4}$

9) $\theta = \frac{3\pi}{8}$, $\varphi = \frac{3\pi}{8}$ 10) $\theta = \frac{\pi}{2}$, $\varphi = 0$ 11) $\theta = \frac{\pi}{2}$, $\varphi = \frac{\pi}{8}$ 12) $\theta = \frac{\pi}{2}$, $\varphi = \frac{\pi}{4}$

13) $\theta = \frac{\pi}{2}$, $\varphi = \frac{3\pi}{8}$ 14) $\theta = \frac{\pi}{2}$, $\varphi = \frac{\pi}{2}$ 15) $\theta = \frac{5\pi}{8}$, $\varphi = 0$ 16) $\theta = \frac{5\pi}{8}$, $\varphi = \frac{\pi}{8}$

17) $\theta = \frac{5\pi}{8}$, $\varphi = \frac{\pi}{4}$ 18) $\theta = \frac{5\pi}{8}$, $\varphi = \frac{3\pi}{8}$ 19) $\theta = \frac{5\pi}{8}$, $\varphi = \frac{\pi}{2}$ 20) $\theta = \frac{5\pi}{8}$, $\varphi = \frac{5\pi}{8}$

21) $\theta = \frac{3\pi}{4}$, $\varphi = 0$ 22) $\theta = \frac{3\pi}{4}$, $\varphi = \frac{\pi}{8}$ 23) $\theta = \frac{3\pi}{4}$, $\varphi = \frac{\pi}{4}$ 24) $\theta = \frac{3\pi}{4}$, $\varphi = \frac{3\pi}{8}$

25) $\theta = \frac{3\pi}{4}$, $\varphi = \frac{\pi}{2}$ 26) $\theta = \frac{3\pi}{4}$, $\varphi = \frac{5\pi}{8}$ 27) $\theta = \frac{3\pi}{4}$, $\varphi = \frac{3\pi}{4}$ 28) $\theta = \frac{7\pi}{8}$, $\varphi = 0$

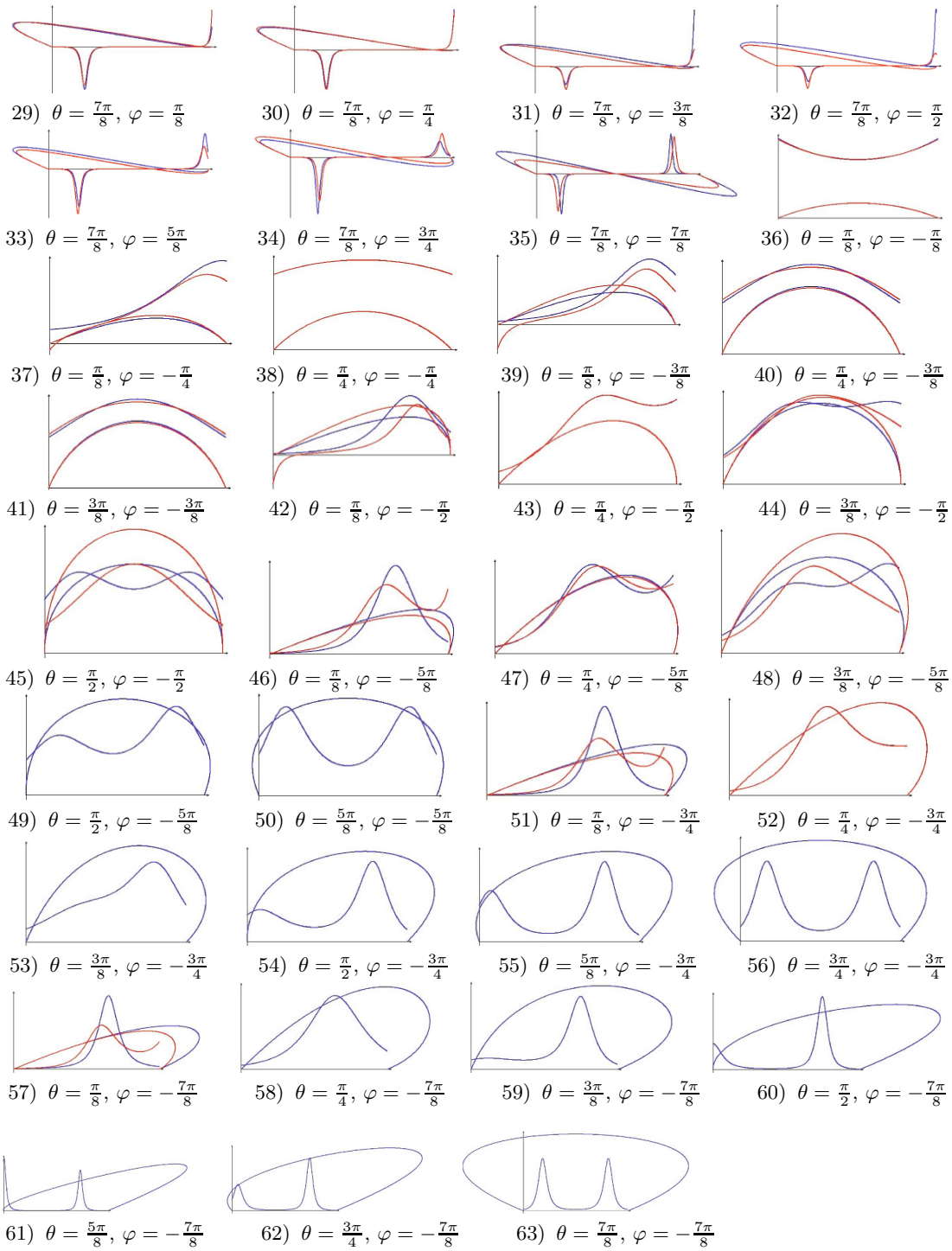

29) $\theta=\frac{7\pi}{8}$, $\varphi=\frac{\pi}{8}$ 30) $\theta=\frac{7\pi}{8}$, $\varphi=\frac{\pi}{4}$ 31) $\theta=\frac{7\pi}{8}$, $\varphi=\frac{3\pi}{8}$ 32) $\theta=\frac{7\pi}{8}$, $\varphi=\frac{\pi}{2}$

33) $\theta=\frac{7\pi}{8}$, $\varphi=\frac{5\pi}{8}$ 34) $\theta=\frac{7\pi}{8}$, $\varphi=\frac{3\pi}{4}$ 35) $\theta=\frac{7\pi}{8}$, $\varphi=\frac{7\pi}{8}$ 36) $\theta=\frac{\pi}{8}$, $\varphi=-\frac{\pi}{8}$

37) $\theta=\frac{\pi}{8}$, $\varphi=-\frac{\pi}{4}$ 38) $\theta=\frac{\pi}{4}$, $\varphi=-\frac{\pi}{4}$ 39) $\theta=\frac{\pi}{8}$, $\varphi=-\frac{3\pi}{8}$ 40) $\theta=\frac{\pi}{4}$, $\varphi=-\frac{3\pi}{8}$

41) $\theta=\frac{3\pi}{8}$, $\varphi=-\frac{3\pi}{8}$ 42) $\theta=\frac{\pi}{8}$, $\varphi=-\frac{\pi}{2}$ 43) $\theta=\frac{\pi}{4}$, $\varphi=-\frac{\pi}{2}$ 44) $\theta=\frac{3\pi}{8}$, $\varphi=-\frac{\pi}{2}$

45) $\theta=\frac{\pi}{2}$, $\varphi=-\frac{\pi}{2}$ 46) $\theta=\frac{\pi}{8}$, $\varphi=-\frac{5\pi}{8}$ 47) $\theta=\frac{\pi}{4}$, $\varphi=-\frac{5\pi}{8}$ 48) $\theta=\frac{3\pi}{8}$, $\varphi=-\frac{5\pi}{8}$

49) $\theta=\frac{\pi}{2}$, $\varphi=-\frac{5\pi}{8}$ 50) $\theta=\frac{5\pi}{8}$, $\varphi=-\frac{5\pi}{8}$ 51) $\theta=\frac{\pi}{8}$, $\varphi=-\frac{3\pi}{4}$ 52) $\theta=\frac{\pi}{4}$, $\varphi=-\frac{3\pi}{4}$

53) $\theta=\frac{3\pi}{8}$, $\varphi=-\frac{3\pi}{4}$ 54) $\theta=\frac{\pi}{2}$, $\varphi=-\frac{3\pi}{4}$ 55) $\theta=\frac{5\pi}{8}$, $\varphi=-\frac{3\pi}{4}$ 56) $\theta=\frac{3\pi}{4}$, $\varphi=-\frac{3\pi}{4}$

57) $\theta=\frac{\pi}{8}$, $\varphi=-\frac{7\pi}{8}$ 58) $\theta=\frac{\pi}{4}$, $\varphi=-\frac{7\pi}{8}$ 59) $\theta=\frac{3\pi}{8}$, $\varphi=-\frac{7\pi}{8}$ 60) $\theta=\frac{\pi}{2}$, $\varphi=-\frac{7\pi}{8}$

61) $\theta=\frac{5\pi}{8}$, $\varphi=-\frac{7\pi}{8}$ 62) $\theta=\frac{3\pi}{4}$, $\varphi=-\frac{7\pi}{8}$ 63) $\theta=\frac{7\pi}{8}$, $\varphi=-\frac{7\pi}{8}$

References

[1] C de Boor, K Hóllig, M Sabin. *High accuracy geometric Hermite interpolation*, Comput Aided Geom Design, 1987, 4: 269-278.

[2] G Celniker, D Gossard. *Deformable curve and surface finite elements for free form shape design*, Comput Graph, 1991, 25: 257-266.

[3] G Celniker, W Welch. *Linear constraints for deformable B-spline surfaces*, Proc Sympos Interactive 3D Graph, ACM, 1992, 165-170.

[4] J Chi, C Zhang, L Xu. *Constructing geometric Hermite curve with minimum curvature variation*, Ninth International Conference on Computer Aided Design and Computer Graphics in HongKong, 2005, 7-10.

[5] D Emery, W Han. *Minimal-energy splines: I. plane curves with angle constraints*, Math Methods Appl Sci, 1990, 13: 351-372.

[6] E T Y Lee. *Choosing nodes in parametric curve interpolation*, Comput Aided Design, 1989, 21: 363-370.

[7] E H Mansfield. *The Bending and Stretching of Plates*, Machillan, New York, 1964.

[8] H P Moreton, C H Séquin. *Functional optimization for surface design*, Comput Graph, 1992, 26: 167-176.

[9] T F Rida. *The elastic bending energy of pythagorean hodograph curves*, Comput Aided Geom Design, 1996, 13: 227-241.

[10] R F Sarraga. *Recent methods for surface shape optimization*, Comput Aided Geom Design, 1998, 15: 417-436.

[11] D Terzopoulos. *Multilevel computational processes for visual surface reconstruction*, Comput Vision Graph Image Process, 1983, 24: 52-96.

[12] D Terzopoulos, H Qin. *Dynamic NURBS with geometric constraints for interactive sculpting*, ACM Trans Graph, 1994, 13: 103-136.

[13] A C Ugural, S K Ferster. *Advanced strength and applied elasticity*, America Elsevier Publishing Co., New York, 1975.

[14] W Welch, A Witkin. *Variational surface modeling*, Comput Graph, 1992, 26: 157-166.

[15] G Yong, F Cheng. *Geometric Hermite curves with minimum strain energy*, Comput Aided Geom Design, 2004, 21, 281-301.

[16] C Zhang, P Zhang, F Cheng. *Constraint scaling of trimmed NURBS surface based on Fix-and-Strethch approach*, Comput Aided Design, 2001, 33: 103-112.

[17] C Zhang, P Zhang, F Cheng. *Fairing spline curves and surfaces by minimizing energy*, Comput Aided Design, 2001, 33: 913-923.

[1] School of Computer Science and Technology, Shandong University, Jinan 250101, China.
Email: xmli@sdu.edu.cn

[2] Shandong Province Key Lab of Digital Media Technology, Shandong University of Finance and Economics, Jinan 250061, China.